JOURNAL OF COMPUTATIONAL PHYSICS 122, 231–243 (1995)

On Nonreflecting Boundary Conditions

MARCUS J. GROTE* AND JOSEPH B. KELLER†

Stanford University, Stanford, California 94305

Received October 24, 1994; revised March 22, 1995

Improvements are made in nonreflecting boundary conditions at artificial boundaries for use with the Helmholtz equation. First, it is shown how to remove the difficulties that arise when the exact DtN (Dirichlet-to-Neumann) condition is truncated for use in computation, by modifying the truncated condition. Second, the exact DtN boundary condition is derived for elliptic and spheroidal coordinates. Third, approximate local boundary conditions are derived for these coordinates. Fourth, the truncated DtN condition in elliptic and spheroidal coordinates is modified to remove difficulties. Fifth, a sequence of new and more accurate local boundary conditions is derived for polar coordinates in two dimensions. Numerical results are presented to demonstrate the usefulness of these improvements.

1. INTRODUCTION

To solve an equation in an infinite domain numerically, it is usual to limit the computation to a finite domain Ω. This requires a boundary condition on the outer boundary S of Ω, which is often called an artificial boundary. It is desirable that this condition be such that the solution of the problem in Ω is exactly the restriction to Ω of the solution of the original problem in the infinite domain. Such a boundary condition is called an exact nonreflecting boundary condition because it permits waves in Ω to travel outward without any spurious reflection from the artificial boundary. An exact nonreflecting boundary condition, the DtN (Dirichlet-to-Neumann) condition, was derived by Keller and Givoili [1] for the Helmholtz equation when the artificial boundary is a circle or sphere. It is a nonlocal condition, and it involves an infinite trigonometric or spherical harmonic series. In practice the infinite series in the DtN condition is truncated at a finite number of terms, and it is then no longer exact.

Our first goal is to modify the truncated DtN condition to make it more accurate and to eliminate the real eigenvalues of the problem in Ω which may make that problem difficult or impossible to solve. Our second goal is to derive the DtN condition for elliptic and spheroidal artificial boundaries. Third, we shall derive approximate local boundary conditions for elliptic and spheroidal coordinates, which are the analogues of the Bayliss–Gunzburger–Turkel (BGT) [2] boundary conditions in polar and spherical coordinates. Fourth, we shall modify the truncated versions of the DtN conditions for elliptic and spheroidal boundaries. Fifth, we shall present a sequence of local boundary conditions in two-dimensional polar coordinates, which are much more accurate than the BGT conditions at low frequencies and equally accurate at high frequencies.

The DtN condition is of the form $\partial_r U = MU$, where M is a nonlocal operator acting on the value of U on the artificial boundary. In the truncated condition $\partial_r U = M^N U$, only modes with mode number $n \leq N$ are retained in $M^N U$. Consequently for the modes with $n > N$ the truncated condition is just $\partial_r U = 0$, which is the source of the real eigenvalues of the problem in Ω. The effect of these eigenvalues can be avoided by choosing N large enough, as Harari and Hughes [3] have shown, when S is a circle or sphere. However, this requires the use of a large number of modes when the frequency is high or the radius of the circle or sphere is large.

There is a much simpler way to remove these difficulties, as we shall show. It is to replace the condition $\partial_r U = 0$ on the modes above N by another condition, such as the Sommerfeld condition $\partial_r U = ikU$ or one of the BGT conditions. We shall see that this modification removes the difficulty due to real eigenvalues and decreases the error. Furthermore, the effort required to implement any such modification is minimal. We call the new condition the modified DtN boundary condition.

We can also view the new boundary condition as a modification of the Sommerfeld condition or of one of the BGT conditions. These conditions tend to be accurate for large values of ka but inaccurate for small values of ka. Here k is the wave number in the Helmholtz equation and a is the radius of the artificial boundary. To correct them for ka small, we modify them by imposing the DtN condition on the modes with $n \leq N$. The resulting boundary condition is just the modified DtN condition.

2. THE DtN FORMULATION

Let $\mathcal{R}$ be a bounded domain in $d = 2$ or $d = 3$ space dimensions, and let Γ be its piecewise smooth boundary. We

* E-mail: grote@cims.nyu.edu.

† keller@math.stanford.edu. This work was supported in part by AFOSR, NSF, and ONR.

0021-9991/95 $12.00

seek the solution of the Helmholtz equation in the region exterior to $\mathcal{R}$, satisfying some boundary condition on Γ and satisfying the Sommerfeld radiation condition at infinity. The boundary value problem for U is

$$\Delta U + k^2 U = f \quad \text{outside } \mathcal{R} \tag{2.1}$$

$$\alpha U + \beta \frac{\partial U}{\partial n} = g \text{ on } \Gamma \tag{2.2}$$

$$\lim_{r\to\infty} r^{(d-1)/2}\left(\frac{\partial U}{\partial r} - ikU\right) = 0. \tag{2.3}$$

Here k is the wave number, f is a source term, and α, β, and g are functions defined on Γ. We assume that the source term f has compact support.

We now surround the object $\mathcal{R}$ and the support of f by an artificial circular or spherical boundary S of radius a. The computational domain Ω is the region inside S and exterior to $\mathcal{R}$. To solve (2.1)–(2.3) in Ω, we must impose a boundary condition on $r = a$. It should be such that the solution of (2.1)–(2.3) with this artificial boundary condition coincides with the restriction to Ω of the solution in the infinite domain. Keller and Givoli [1] derived such a boundary condition and called it the DtN map, because it relates Dirichlet to Neumann data at $r = a$. It takes the general form

$$\partial_r U = MU, \quad r = a. \tag{2.4}$$

This condition is global on the artificial boundary. In two dimensions it is

$$\partial_r U(a, \theta) = \frac{1}{\pi}\sum_{n=0}^{\infty}{}' \frac{kH_n^{(1)\prime}(ka)}{H_n^{(1)}(ka)} \int_0^{2\pi} \cos n(\theta - \theta') U(a, \theta')\, d\theta'. \tag{2.5}$$

Here $H_n^{(1)}$ is the Hankel function of the first kind of order n, and the prime after the sum indicates that the term with $n = 0$ is multiplied by $\frac{1}{2}$. The corresponding condition for three dimensions is given by (4.15).

The solution of (2.1) and (2.2) in Ω with (2.4) at $r = a$ is unique and coincides with the restriction to Ω of the solution of (2.1)–(2.3). This follows from the fact that any solution of (2.1), (2.2), and (2.4) within Ω can be continued into a solution of (2.1)–(2.3) and from the uniqueness of the solution of (2.1)–(2.3). It was also shown directly by Harari and Hughes [3].

3. THE MODIFIED DtN CONDITION: THEORY

In practice (2.5) must be approximated by truncating the series at a finite value N. We denote the truncated DtN map by M^N, and we replace (2.4) by

$$\partial_r U = M^N U, \quad r = a. \tag{3.1}$$

Then the new problem is (2.1), (2.2), and (3.1).

Equation (3.1) is exact for the low modes, $0 \le n \le N$, but it imposes the incorrect condition $\partial_r U = 0$ at $r = a$ on all higher modes. As a consequence the new problem will have an infinite sequence of real eigenvalues $k_j^2 \ge 0$, $j = 1, 2, \ldots$, when α/β is real. When k^2 is such an eigenvalue, the new problem will not have a solution unless f satisfies certain solvability conditions, and if it does have a solution, it is not unique. Harari and Hughes [3] showed that this difficulty can be eliminated by choosing $N \ge ka$. This restriction on ka for a fixed value of N is an artifact of the truncation. Moreover, it could require including many more terms in the DtN map than may actually be necessary to achieve a desired accuracy. It may also create a large overhead in computation, especially in three dimensions. We shall now demonstrate how to overcome this difficulty and simultaneously improve upon the accuracy of the solution with the truncated DtN boundary condition, without any restriction on ka.

Let B denote a linear operator, such that (2.1), (2.2), and $\partial_r U = BU$ at $r = a$ is a well-posed problem. One example of such an operator is $B = ik$, which occurs in the Sommerfeld condition. We shall apply B to the higher modes, without modifying the exact boundary condition on the lower modes. To do so, we simply add and subtract BU on the right side of (2.4) and then truncate $M - B$. This yields the modified DtN condition

$$\partial_r U = (M^N - B^N)U + BU, \quad r = a. \tag{3.2}$$

The boundary condition (3.2) coincides with (2.4) and (3.1) for all modes up to N. However, on all higher modes (3.2) is $\partial_r U = BU$. We shall now present a condition on B which is *sufficient* to ensure the well-posedness of the problem (2.1), (2.2), and (3.2), regardless of the wave number k, the point of truncation N, or the shape of the obstacle Γ.

THEOREM 3.1. *Let B be a linear operator that acts on the values of U on the outer boundary $r = a$ such that*

$$\operatorname{Im} \int_{r=a} \overline{v}\, Bv\, ds > 0 \quad \forall v \ne 0. \tag{3.3}$$

Then in Ω (2.1), (2.2), and (3.2) have a unique solution.

The same conclusion holds in elliptic or spheroidal coordinates, with S defined by $\mu = a$ and r replaced by μ in (3.2).

Proof. Let U be a solution of (2.1), (2.2), and (3.2), with $f = 0$ and $g = 0$. We must show that U is the trivial solution $U = 0$ in Ω. To do so, we multiply (2.1) by $\overline{U}$, the complex conjugate of U, and integrate over Ω. Using integration by parts and the homogeneous boundary condition on Γ, we obtain

$$\int_\Omega [\|\nabla U\|^2 - k^2|U|^2]\, d\Omega - \int_{r=a} [\overline{U}(M^N - B^N)U + \overline{U}BU]\, ds = 0. \tag{3.4}$$

Taking the imaginary part of (3.4) yields

$$\operatorname{Im} \int_{r=a} [\overline{U}(M^N - B^N)U + \overline{U}BU]\, ds = 0. \tag{3.5}$$

On $r = a$ let $U = U_{\leq} + U_{>}$, where $U_{\leq}$ is the sum of the modes numbered $n \leq N$, and $U_{>}$ is the sum of the modes numbered above N. Because the modes are mutally orthogonal with respect to the L_2 inner product on $r = a$, we can rewrite (3.5) as

$$\operatorname{Im} \int_{r=a} [\overline{U}_{\leq} M^N U_{\leq} + \overline{U}_{>} B U_{>}]\, ds = 0. \tag{3.6}$$

For simplicity, we now consider the two-dimensional case. We compute explicitly the first expression in (3.6), using (2.5), to get

$$\begin{aligned} \operatorname{Im} \int_{r=a} & \overline{U}_{\leq} M^N U_{\leq}\, ds \\ &= \sum_{n=0}^{N} \operatorname{Im} \alpha_n \left\{ \left| \int_0^{2\pi} U(a, \theta') \cos n\theta'\, d\theta' \right|^2 \right. \\ &\quad \left. + \left| \int_0^{2\pi} U(a, \theta') \sin n\theta'\, d\theta' \right|^2 \right\}. \end{aligned} \tag{3.7}$$

Here

$$\alpha_n = \frac{kH_n^{(1)\prime}(ka)}{H_n^{(1)}(ka)}. \tag{3.8}$$

We write $H_n^{(1)} = J_n + iY_n$ in (3.7) and use the fact that the Wronskian of $J_n(ka)$ and $Y_n(ka)$ is equal to $2/\pi ka$. Then we find that the imaginary part of α_n is given by

$$\operatorname{Im} \alpha_n = \frac{2}{\pi a |H_n^{(1)}(ka)|^2} > 0. \tag{3.9}$$

From (3.7) and (3.9) it follows that the first term in (3.6) is positive unless $U_{\leq} = 0$. Similarly, (3.3) shows that the second term in (3.6) is positive unless $U_{>} = 0$. Thus (3.6) implies that $U = U_{\leq} + U_{>} = 0$ on $r = a$. Since B and M^N involve only the values of U on $r = a$, we infer from the boundary condition (3.2) that $\partial_r U = 0$ on $r = a$. Since U is analytic in Ω, this implies that U is identically zero in Ω. ∎

The hypothesis of Theorem 3.1 clearly holds when the operator B is a constant with a positive imaginary part. For the Sommerfeld condition $\partial_r U = ikU$ and the first-order BGT conditions, given by (4.2) for the circle and (4.11) for the sphere, both with $m = 1$, the imaginary part of the constant operator B is equal to k. For the first-order local conditions, given by (4.27) for the ellipse and by (4.49) for the spheroid, both with $m = 1$, the imaginary part of B is $kf \sinh a$, where $f > 0$. Therefore Im B is positive. Hence, the problem (2.1), (2.2), and the modified DtN condition (3.2) with any one of these five boundary operators is well-posed for any obstacle and any wave number, regardless of the point of truncation N. However, the condition (3.3) is not satisfied by the second-order BGT condition (4.2) with $m = 2$, when S is a circle.

Although Theorem 3.1 applies to any obstacle Γ, it requires that B satisfy (3.3). When Γ is a circle or sphere of radius b, the conclusion of Theorem 3.1 follows without (3.3). To prove it we write $U = U_{\leq} + U_{>}$ throughout the entire annulus $b \leq r \leq a$ and suppose that U satisfies the homogeneous form of (2.1), (2.2), and (3.2). Then $U_{\leq}$ satisfies the homogeneous problem with the DtN condition (2.4) on $r = a$, so $U_{\leq} = 0$. Similarly, $U_{>}$ satisfies the homogeneous problem with $\partial_r U_{>} = BU_{>}$ on $r = a$, so $U_{>} = 0$ by assumption. This implies that $U = 0$. Thus we have proved the following theorem.

THEOREM 3.2. *Let $\Gamma \subset \Omega$ be a circle in two dimensions or a sphere in three dimensions. Suppose that the solution of* (2.1) *and* (2.2) *with $\partial_r U = BU$ on $r = a$ is unique. Then* (2.1) *and* (2.2) *with the modified DtN condition* (3.2) *is unique for all $N \geq 0$.*

The same conclusion holds in elliptic or spheroidal coordinates, with S defined by $\mu = a$ and r replaced by μ in (3.2).

As an application of Theorem 3.2, let us choose $B = \partial_r + B_2$, where B_2 is the second BGT operator defined in (4.11) with $m = 2$. In [2] it was shown that (2.1) and (2.2), with $B_2 U = 0$ on $r = a$, is well-posed for Γ a sphere. Theorem 3.2 shows that the problem remains well-posed when the modified DtN condition (3.2) is used with $B = B_2 + \partial_r$.

This theorem holds when Γ is a circle, sphere, ellipse, or spheroid, which is a limited class of obstacles. Of course, the most important applications of the DtN and the modified DtN boundary conditions are to obstacles Γ, which are not separable coordinate surfaces. Theorem 3.1 applies to such Γ for a restricted class of boundary operators. Theorem 3.2 suggests that uniqueness may hold for a more general class of boundary operators.

A typical solution using the DtN boundary condition in prolate spheroidal coordinates is shown in Fig. 1.

4. THE MODIFIED DtN CONDITION: APPLICATIONS

4.1. *General Method*

Now we shall derive modified DtN boundary conditions for the following four artificial boundaries: the circle, the sphere, the ellipse, and the prolate spheroid. In each case we begin with a particular local operator B, and then we use it to derive (3.2) for the geometry considered. To obtain B, we proceed as in [2] and construct a differential operator B_m that annihilates the first m terms in the large distance expansion of any solution U. We note that this expansion is convergent in three dimen-

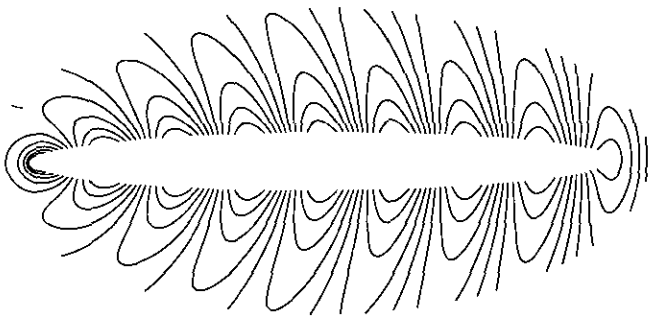

FIG. 1. Contour lines of Re U_h^s are shown for the scattering of a plane wave incident from the right, by the prolate spheroid $\mu = 0.1$ of aspect ratio 10 : 1, with $k = 4\pi$. The numerical solution is computed using the DtN boundary condition (4.46) with $N = 15$, and the artificial boundary S is the spheroid $\mu = 0.5$.

sions, but only asymptotic in two dimensions. In Section 5 we derive an improved local boundary condition in the circular case by using a convergent, instead of an asymptotic, expansion.

We shall then compare the accuracy of the various boundary conditions through a series of numerical experiments. In each one of them we consider the scattering of an incident plane wave U^i impinging upon one of the following obstacles: a circular cylinder, an elliptic cylinder, a sphere, and a prolate spheroid. On the surface of the obstacle we impose the acoustically soft boundary condition $U = U^i + U^s = 0$. The exact solution for the scattered field U^s is computed using a plane wave expansion [4]. Because of the inherent symmetry of each problem, it is sufficient to compute the solution for $0 \le \theta \le \pi$, with the boundary condition $\partial_\theta U = 0$ on $\theta = 0$ and $\theta = \pi$. In all cases, the numerical solution is computed using a second-order centered finite difference discretization. The grid is evenly spaced with 40 intervals in r or μ and 240 in $0 \le \theta \le \pi$. The grid is fine enough to ensure that when a local boundary condition is used, the error is essentially due to the imposition of the boundary condition, and it is not due to the discretization error of the finite difference approximation.

At any mesh point on S, the centered finite difference approximations to the radial derivatives that appear in (2.1) involve one unknown, which lies outside of Ω. Since it also appears in the centered finite difference approximation to the nonreflecting boundary condition, we can eliminate it from the linear system of equations. The inner products along the outer boundary are computed using Simpson's fourth-order quadrature rule. The solution U_h^s of the resulting complex linear system is computed in double precision FORTRAN with a banded direct solver from LAPACK. We validated our code in the circular case by comparing our results with those obtained using the Matlab implementation of Ernst [5].

The error is always computed in the maximum (or L-infinity) norm over the entire domain Ω and normalized with respect to the exact solution:

$$\text{error} = \frac{\|U_h^s - U^s\|_\infty}{\|U^s\|_\infty}. \tag{4.1}$$

We note that the relative and absolute errors coincide because the maximal modulus of the solution U^s always occurs on the surface of the obstacle, where it is equal to one. The DtN and modified DtN conditions require the computation of some special functions, such as Hankel, Mathieu, or spheroidal wave functions. The work required to compute them is negligible compared to the work in solving the linear system.

4.2. *The Circular Case*

We begin with polar coordinates in two dimensions r, θ with the outer boundary located at $r = a$. The sequence of local operators B_m derived in [2] is

$$B_m = \prod_{l=1}^{m} \left(\frac{\partial}{\partial r} - ik + \frac{4l-3}{2r} \right). \tag{4.2}$$

where $l = 1$ is the rightmost term in the product. The boundary condition on $r = a$ is

$$B_m U = 0, \quad r = a. \tag{4.3}$$

By setting $B = B_m + \partial_r$, we can rewrite (4.3) in the generic form

$$\partial_r U = BU, \quad r = a. \tag{4.4}$$

We can now use B in (3.2) to modify the DtN boundary condition.

To obtain the modified DtN condition using B_1, we write (4.4) with $m = 1$ as

$$\partial_r U(a, \theta) = \left(ik - \frac{1}{2a} \right) U(a, \theta). \tag{4.5}$$

Next, on the right side of (2.5) we add and subtract $(ik - 1/2a)U$, and include the subtracted term in the sum. Truncating the series at N yields the modified DtN condition:

$$\begin{aligned} \partial_r U(a, \theta) = &\left(ik - \frac{1}{2a} \right) U(a, \theta) \\ &+ \frac{1}{\pi} {\sum_{n=0}^{N}}' \left(\frac{kH_n^{(1)\prime}(ka)}{H_n^{(1)}(ka)} - ik + \frac{1}{2a} \right) \\ &\int_0^{2\pi} \cos n(\theta - \theta') U(a, \theta')\, d\theta'. \end{aligned} \tag{4.6}$$

When $m = 2$, the analysis is similar but slightly more involved. First we rewrite $B_2 U = 0$ given by (4.2) with $m = 2$ as

$$\partial_r U(a, \theta) = \left(\frac{3}{4a} - k^2 a - 3ik + (4 - 2ika)\partial_\tau + a\partial_\tau^2 \right) U(a, \theta). \tag{4.7}$$

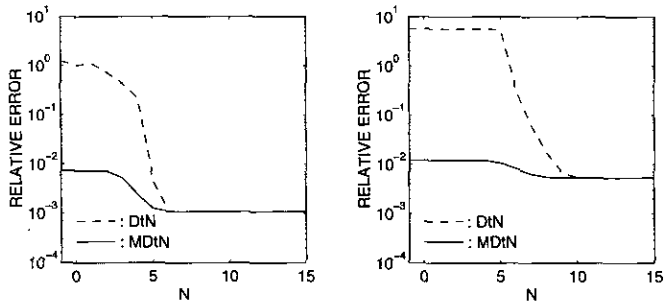

FIG. 2. Scattering of a plane wave from the infinite circular cylinder $r = 0.5$. The artificial boundary is located at $r = 1$. The relative error (4.1) is shown versus the truncation point N in the boundary conditions (2.5) and (4.9): left, $k = 2\pi$; right, $k = 4\pi$.

Next we add and subtract (4.7) from the right side of (2.5). Since $H_n^{(1)}$ satisfies Bessel's equation

$$H_n^{(1)\prime\prime} + \frac{1}{z} H_n^{(1)\prime} + \left(1 + \frac{n^2}{z^2}\right) H_n^{(1)} = 0, \tag{4.8}$$

we can express $H_n^{(1)\prime\prime}$ in terms of first- and zeroth-order derivatives. Then we truncate the series at N to obtain the modified DtN condition,

$$\begin{aligned} \partial_r U(a, \theta) = &\left(\frac{3}{4a} - k^2 a - 3ik + (4 - 2ika)\partial_\tau + a\partial_\tau^2\right) U(a, \theta) \\ &+ \frac{1}{\pi} \sum_{n=0}^{N}{}' Z_n \int_0^{2\pi} \cos n(\theta - \theta') U(a, \theta')\, d\theta', \end{aligned} \tag{4.9}$$

where the constants Z_n are given by

$$Z_n = 2(ika - 1)\frac{kH_n^{(1)\prime}(ka)}{H_n^{(1)}(ka)} + \frac{1}{a}\left(2k^2a^2 - \frac{3}{4} - n^2 + 3ika\right). \tag{4.10}$$

It is to be expected that (4.9), employing B_2, will be more accurate than (4.6), employing B_1, and we have performed numerical computations which verify this. Furthermore, it is not much harder to implement B_2 than B_1. Therefore, we shall now illustrate the accuracy of (4.9), based upon B_2.

To test the accuracy of the boundary condition (4.9), we consider the scattering of an incoming plane wave $U^i = e^{ikx}$. It impinges upon an infinite circular cylinder whose cross section is a circle of radius $r = 0.5$ in the xy-plane. We choose the outer boundary to be the circle $r = 1$ and solve the resulting problem as described in Section 4.1. In Fig. 2 we compare the relative error (4.1) obtained by using the DtN condition (2.5) truncated at N with that obtained by using the second modified DtN (MDtN) condition (4.9) for different values of N. We choose $k = 2\pi$ and $k = 4\pi$ and apply the boundary condition for increasing values of N. The sum is truncated at N, which is included in the sum. Thus for $N = -1$, the sum completely vanishes and (2.5) reduces to $\partial_r U(a, \theta) = 0$, whereas (4.9) reduces to $B_2 U = 0$. We see that for small values of N the error in using the truncated DtN operator remains very large because of the spurious eigenmodes. When N is large enough so that the DtN map captures the main harmonic modes present in the solution, the error quickly reaches its lowest value for the given grid. The modified DtN condition, however, yields an acceptable accuracy even for small values of N, since it merely improves upon the local boundary condition used to modify it. This is an advantage, since it is usually not known in advance how high N must be to reach a desired accuracy. Setting $N \geq ka$ merely ensures well-posedness, but it does not guarantee optimal accuracy on the underlying grid. For large values of N, the error for $k = 2\pi$ is smaller than the error for $k = 4\pi$, because we have used the same grid for both computations. Indeed, at very large values of N, the error is mainly due to the finite resolution of the grid. For small values of N, the boundary condition behaves like a local boundary condition. For local boundary conditions, the dependence of the error on k is shown in Fig. 6.

4.3. *The Spherical Case*

We consider the polar coordinate system r, θ, ϕ in three space dimensions, related to the rectangular coordinate system by $x = r \cos\theta \cos\phi$, $y = r \cos\theta \sin\phi$, and $z = r \cos\theta$. Hence, the positive z-axis coincides with $\theta = 0$ and the negative z-axis with $\theta = \pi$. The local operator B_m derived in [2] is

$$B_m = \prod_{l=1}^{m} \left(\frac{\partial}{\partial r} - ik + \frac{2l-1}{r}\right), \tag{4.11}$$

where $l = 1$ is the rightmost term in the product. Next, we introduce the notation

$$m_n(\theta, \phi, \theta', \phi') = \sum_{j=0}^{n}{}' \beta_{jn} P_n^j(\cos\theta) P_n^j(\cos\theta') \cos j(\phi - \phi'). \tag{4.12}$$

Here the prime after the sum indicates that the term with $j = 0$ is multiplied by $\frac{1}{2}$. The constants β_{nj} are defined by

$$\beta_{nj} = \frac{(2n+1)(n-j)!}{2\pi(n+j)!}. \tag{4.13}$$

The solution of the exterior radiation problem can then be written as

$$\begin{aligned} &U(r, \theta, \phi) \\ &= \sum_{n=0}^{\infty} \sqrt{\frac{a}{r}} \frac{H_{n+1/2}^{(1)}(kr)}{H_{n+1/2}^{(1)}(ka)} \int_{\mathcal{S}} m_n(\theta, \phi, \theta', \phi') U(a, \theta', \phi')\, d\mathcal{S}'. \end{aligned} \tag{4.14}$$

Here $d\mathcal{S}' = \sin\theta'\, d\phi'\, d\theta'$ denotes the differential surface element on the unit sphere $\mathcal{S}$. We differentiate (4.14) with respect to r and set $r = a$ to obtain the DtN condition

$$\partial_r U(a, \theta, \phi) = \sum_{n=0}^{\infty} \left[\frac{kH_{n+1/2}^{(1)\prime}(ka)}{H_{n+1/2}^{(1)}(ka)} - \frac{1}{2a} \right] \int_{\mathcal{S}} m_n(\theta, \phi, \theta', \phi') U(a, \theta', \phi')\, d\mathcal{S}'. \tag{4.15}$$

To obtain the modified DtN condition for $m = 1$, we simply rewrite (4.3) at $r = a$ as $\partial_r U = (ik - 1/a)U$, with B_1 given by (4.11). Then we add and subtract $(ik - 1/a)U$ on the right side of (4.15) and include the subtracted term in the sum. Finally, we truncate the sum at N to get

$$\partial_r U(a, \theta, \phi) = \left(ik - \frac{1}{a} \right) U(a, \theta, \phi) + \sum_{n=0}^{N} \left[\frac{kH_{n+1/2}^{(1)\prime}(ka)}{H_{n+1/2}^{(1)}(ka)} - ik - \frac{1}{a} \right] \int_{\mathcal{S}} m_n(\theta, \phi, \theta', \phi') U(a, \theta', \phi')\, d\mathcal{S}'. \tag{4.16}$$

To derive the second modified DtN condition, we set

$$BU = (a\partial_r^2 - 2ika\partial_r + 5\partial_r - 4ik - k^2 a + 2/a)U \tag{4.17}$$

and rewrite $B_2 U = 0$ as $\partial_r U = BU$ at $r = a$. Next, we add and subtract BU on the right side of (4.15) and include the subtracted term in the sum. To do so, we need to compute $-BH_{n+1/2}^{(1)}(kr)/\sqrt{r}$ at $r = a$ and replace second-order derivatives by zeroth- and first-order derivatives of $H_{n+1/2}^{(1)}$, using (4.8) with n replaced by $n + \frac{1}{2}$. After some algebra this yields the modified DtN condition

$$\partial_r U(a, \theta, \phi) = \left(a\partial_r^2 - 2ika\partial_r + 5\partial_r - 4ik - k^2 a + \frac{2}{a} \right) U(a, \theta, \phi) + \sum_{n=0}^{N} Z_n \int_{\mathcal{S}} m_n(\theta, \phi, \theta', \phi') U(a, \theta', \phi')\, d\mathcal{S}', \tag{4.18}$$

with the constants Z_n given by

$$Z_n = 2k(ika - 1) \frac{H_{n+1/2}^{(1)\prime}(ka)}{H_{n+1/2}^{(1)}(ka)} + (3ika + 2(ka)^2 - n^2 - n - 1)/a. \tag{4.19}$$

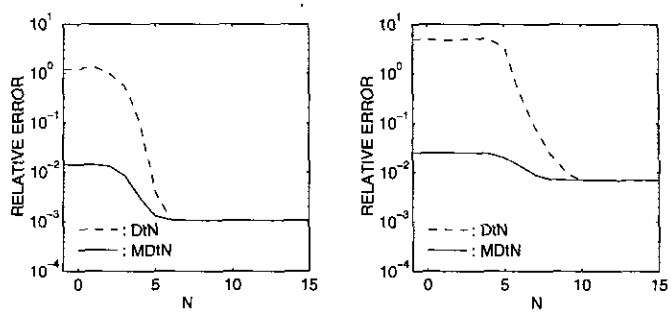

FIG. 3. Scattering of a plane wave from the sphere $r = 0.5$. The artificial boundary is located at $r = 1$. The relative error (4.1) is shown versus the number N of terms retained in the boundary conditions (4.15) and (4.18): left, $k = 2\pi$; right, $k = 4\pi$.

We now consider the scattering of a plane wave $U^i = e^{ikz}$ from a sphere of radius $r = 0.5$. Because the z-axis coincides with the direction of propagation, we take advantage of the axisymmetry of the problem. It can be solved in the two-dimensional region $0.5 \le r \le 1$, $0 \le \theta \le \pi$, with $\partial_\theta U = 0$ on $\theta = 0$ and $\theta = \pi$. In Fig. 3 we compare the relative error obtained by using the DtN condition (4.15) truncated at N with that obtained by using the modified DtN condition (4.18) for different values of N. For $N = -1$, the DtN condition reduces to $\partial_r U = 0$, whereas the modified DtN condition reduces to (4.3) with B_2 given by (4.11). Again we observe the expected higher accuracy of the modified DtN condition for small values of N.

4.4. *The Elliptic Case*

We now consider the more general case of an elliptic artificial boundary, which can accomodate highly elongated obstacles. The elliptic coordinates μ, θ are related to the rectangular Cartesian coordinates x, y by

$$x = f \cosh\mu \cos\theta, \quad y = f \sinh\mu \sin\theta. \tag{4.20}$$

Thus, for a constant value of μ, x and y describe a confocal ellipse with foci located at $(-f, 0)$ and $(+f, 0)$. If we let $\xi = \cosh\mu$, the eccentricity of the ellipse is ξ^{-1} and the ratio of major axis to minor axis is equal to $\xi/\sqrt{\xi^2 - 1}$. Next, we set $\sqrt{q} = kf/2$, and let $\mu = a$ denote the outer boundary on which we seek the DtN condition.

We denote $Mc_r^{(3)}(\mu, q)$, $r = 0, 1, \ldots$, and $Ms_r^{(3)}(\mu, q)$, $r = 1, 2, \ldots$, the (radial) Mathieu–Hankel functions [6]. The angular functions $ce_r(\theta, q)$ and $se_r(\theta, q)$ satisfy Mathieu's equation

$$\frac{d^2 y}{d\theta^2} + (\lambda - 2q\cos 2\theta)\, y = 0, \tag{4.21}$$

with the separation constant λ denoted by a_r and b_r for ce_r and se_r, respectively. They form a complete orthogonal set over the interval $0 \le \theta \le 2\pi$ and are normalized such that

$$\int_0^{2\pi} [ce_r(\theta, q)]^2\, d\theta = \int_0^{2\pi} [se_r(\theta, q)]^2\, d\theta = \pi. \tag{4.22}$$

The radial functions $Mc_r^{(3)}$ and $Ms_r^{(3)}$ satisfy Mathieu's modified differential equation

$$\frac{d^2y}{d\mu^2} - (\lambda - 2q\cosh 2\mu)\, y = 0, \tag{4.23}$$

with the separation constant λ denoted by a_r and b_r for $Mc_r^{(3)}$ and $Ms_r^{(3)}$, respectively.

The solution of the exterior problem $\mu \geq a$ is

$$\begin{aligned} U(\mu, \theta) = {} & \frac{1}{\pi} \sum_{r=0}^{\infty} \frac{Mc_r^{(3)}(\mu, q)}{Mc_r^{(3)}(a, q)}\, ce_r(\theta, q) \int_0^{2\pi} U(a, \theta')ce_r(\theta', q)\, d\theta' \\ & + \frac{1}{\pi} \sum_{r=1}^{\infty} \frac{Ms_r^{(3)}(\mu, q)}{Ms_r^{(3)}(a, q)}\, se_r(\theta, q) \\ & \int_0^{2\pi} U(a, \theta')se_r(\theta', q)\, d\theta'. \end{aligned} \tag{4.24}$$

To derive the DtN map, we simply differentiate (4.24) with respect to μ, and set $\mu = a$. This yields

$$\begin{aligned} \partial_\mu U(a, \theta) = {} & \frac{1}{\pi} \sum_{r=0}^{\infty} \frac{Mc_r^{(3)\prime}(a, q)}{Mc_r^{(3)}(a, q)}\, ce_r(\theta, q) \int_0^{2\pi} U(a, \theta')ce_r(\theta', q)\, d\theta' \\ & + \frac{1}{\pi} \sum_{r=1}^{\infty} \frac{Ms_r^{(3)\prime}(a, q)}{Ms_r^{(3)}(a, q)}\, se_r(\theta, q) \\ & \int_0^{2\pi} U(a, \theta')se_r(\theta', q)\, d\theta'. \end{aligned} \tag{4.25}$$

To modify (4.25) we need a local boundary condition, which we shall impose on the modes beyond the point of truncation. We simply extend to the ellipse the procedure employed in [2] for the circle. We begin with the asymptotic representation of the solution for large μ, which is derived in the Appendix:

$$U(\mu, \theta) \sim \frac{e^{i(kf\cosh\mu)}}{\sqrt{\pi kf\cosh\mu}} \sum_{m=0}^{\infty} \frac{g_m(\theta; k)}{[kf\cosh\mu]^m}. \tag{4.26}$$

We note that (4.26) is *formally* identical to the asymptotic expansion in the polar coordinate case, with r replaced by $f\cosh\mu$. Therefore we replace r by $f\cosh\mu$ in (4.2) and obtain the sequence of local operators,

$$B_m = \prod_l^m \left(\frac{1}{f\sinh\mu}\frac{\partial}{\partial\mu} - ik + \frac{4l-3}{2f\cosh\mu} \right), \tag{4.27}$$

where $l = 1$ is the rightmost term in the product. The operator B_m annihilates the first m terms in (4.26). Therefore for large μ, B_mU has the asymptotic behavior

$$B_mU = \mathbb{O}\left([kf\cosh\mu]^{-(2m+1/2)} \right). \tag{4.28}$$

Thus in elliptic coordinates, the analogue of the BGT boundary condition is

$$B_mU = 0, \tag{4.29}$$

with B_m given by (4.27).

Modifying (4.25) with B_1 is straightforward and similar to the procedure used for the circle. We simply set $B_1U = 0$ at $\mu = a$ and then rewrite it as

$$\partial_\mu U(a, \theta) = (ikf\sinh a - \tfrac{1}{2}\tanh a)\, U(a, \theta). \tag{4.30}$$

Again, we add the right side of (4.30) to (4.25) and then subtract it, and we include the subtracted term in the sums. We then truncate the sums at $r = N$, which yields the first modified DtN boundary condition,

$$\begin{aligned} \partial_\mu U(a, \theta) = {} & (ikf\sinh a - \tfrac{1}{2}\tanh a)\, U(a, \theta) \\ & + \frac{1}{\pi} \sum_{r=0}^{N} Z_r^c ce_r(\theta, q) \int_0^{2\pi} U(a, \theta')\, ce_r(\theta', q)\, d\theta' \\ & + \frac{1}{\pi} \sum_{r=0}^{N} Z_r^s se_r(\theta, q) \int_0^{2\pi} U(a, \theta')se_r(\theta', q)\, d\theta', \end{aligned} \tag{4.31}$$

with

$$Z_r^c = \frac{Mc_r^{(3)\prime}(a, q)}{Mc_r^{(3)}(a, q)} - ikf\sinh a + \frac{1}{2}\tanh a, \tag{4.32}$$

$$Z_r^s = \frac{Ms_r^{(3)\prime}(a, q)}{Ms_r^{(3)}(a, q)} - ikf\sinh a + \frac{1}{2}\tanh a. \tag{4.33}$$

To modify (4.25) using B_2, we set $B_2U = 0$ at $\mu = a$ and cast it into the standard form,

$$\partial_\mu U(a, \theta) = (\partial_\mu^2 + (\alpha + 1)\partial_\mu + \beta)U(a, \theta), \tag{4.34}$$

with

$$\alpha = 3\tanh a - 2ikf\sinh a - \coth a, \tag{4.35}$$

$$\beta = \frac{3}{4}\tanh^2 a - (kf\sinh a)^2 - 3ikf\sinh a\tanh a. \tag{4.36}$$

Next, we add the right side of (4.34) to (4.25) and then subtract it, including the subtracted term in the sums. We replace the second derivatives of $Mc_r^{(3)}$ and $Ms_r^{(3)}$ using (4.23), and we truncate the sums at $r = N$. This gives the second modified DtN condition,

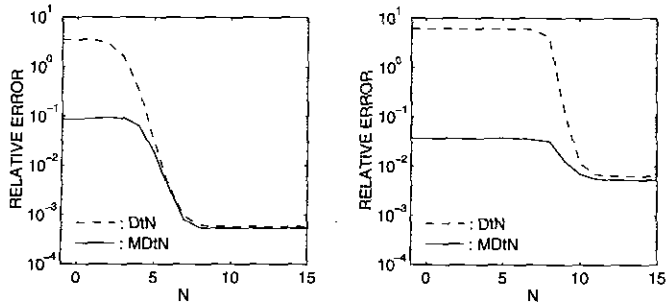

FIG. 4. Scattering of a plane wave from the elliptic cylinder $\mu = 0.1$ of aspect ratio 10 : 1. The artificial boundary is located at $\mu = 0.5$. The relative error (4.1) is shown versus the truncation point N in the boundary conditions (4.25) and (4.37): left, $k = 2\pi$; right, $k = 4\pi$.

$$\partial_\mu U(a, \theta) = (\partial_\theta^2 + (\alpha + 1)\partial_\mu + \beta)\, U(a, \theta) + \frac{1}{\pi}\sum_{r=0}^{N} Z_r^c ce_r(\theta, q) \int_0^{2\pi} U(a, \theta') ce_r(\theta', q)\, d\theta' + \frac{1}{\pi}\sum_{r=1}^{N} Z_r^s se_r(\theta, q) \int_0^{2\pi} U(a, \theta') se_r(\theta', q)\, d\theta', \quad (4.37)$$

with

$$Z_r^c = 2q\cosh 2a - a_r - \beta - \alpha \frac{Mc_r^{(3)\prime}(a, q)}{Mc_r^{(3)}(a, q)}, \quad (4.38)$$

$$Z_r^s = 2q\cosh 2a - b_r - \beta - \alpha \frac{Ms_r^{(3)\prime}(a, q)}{Ms_r^{(3)}(a, q)}. \quad (4.39)$$

We now consider the scattering of a plane wave $U^i = e^{ikx}$ from the infinite elliptic cylinder $\mu = \mu_0$, whose cross section in the xy-plane is a confocal ellipse with foci located at $(\pm 1, 0)$. We set $\mu_0 = 0.1$, so that the aspect ratio of major to minor axes is about 10 : 1, and we choose $a = 0.5$. The propagation direction of the incident wave coincides with the major axis of the ellipse. The characteristic values and Fourier coefficients of the Mathieu functions are computed using code described in [7] and available from Netlib. The radial functions $Mc_r^{(3)}$ and $Ms_r^{(3)}$ are calculated using rapidly converging series in products of Bessel functions [6] and were checked for accuracy against [8]. In Fig. 4 we compare the relative error obtained by using the modified DtN condition (4.37) for different values of N. For $N = -1$, the DtN condition reduces to $\partial_\mu U = 0$, whereas the modified DtN condition reduces to (4.29) with B_2 given by (4.27). Again we observe the expected higher accuracy of the modified DtN condition for small values of N. The error using the truncated DtN condition is large as long as N is small, but it then decreases very rapidly to its optimal value. This behavior is, of course, problem dependent. The discrepancy between the solutions with the DtN and the modified DtN conditions for large values of N is due to the fact that we have replaced the differential operator B_2 by a finite difference approximation. It is negligible in the sense that it lies within the range of the discretization error and is clearly overemphasized by the logarithmic scale.

Next, we vary the aspect ratio of the elliptic cross section of the obstacle $\mu = \mu_0$. In Table I we compare the performance of various boundary conditions for the two aspect ratios 10 : 1 and 2 : 1. The relative error is computed over the region $\mu_0 \le \mu \le \mu_0 + 0.1$, and the mesh size $\Delta\mu$ remains constant as the artificial boundary $\mu = a$ gets closer to the obstacle. The relative error when the DtN condition (4.25) is used remains smaller than 0.075% regardless of the location of the artificial boundary and the shape of the obstacle. The local boundary conditions (4.29), however, perform rather poorly in the highly elongated case $\mu_0 = 0.1$. Their accuracy improves as the artificial boundary moves away from the obstacle.

4.5. *The Prolate Spheroidal Case*

We now present the DtN condition and its modified versions in prolate spheroidal coordinates. This coordinate system accommodates elongated cigar-shaped obstacles. Let μ, θ, ϕ be the prolate spheroidal coordinates related to Cartesian coordinates x, y, z by

$$x = f\cosh\mu\cos\theta, \quad y = f\sinh\mu\sin\theta\cos\phi, \quad z = f\sinh\mu\sin\theta\sin\phi. \quad (4.40)$$

Here $0 \le \theta \le \pi$, $0 \le \phi < 2\pi$, and $\mu \ge 0$. Thus, a surface of constant μ is an ellongated ellipsoid of revolution with major axis of length $2f\cosh\mu$. Surfaces of constant θ are two-sheeted confocal hyperboloids of revolution, and surfaces of constant ϕ are planes containing the major axis, which coincides with the x-axis. We set $c = kf$ and $\xi = \cosh\mu$ and denote by $R_{mn}^{(3)}(c, \xi)$ the radial prolate spheroidal wave functions of the third kind [6, 9]. They satisfy

TABLE I

Scattering of a Plane Wave from the Elliptic Cylinder $\mu = \mu_0$ with $k = 2\pi$

	$\mu_0 = 0.1$, Aspect ratio 10 : 1		$\mu_0 = 0.5$, Aspect ratio 2 : 1	
$\mu = a$	$a = 0.2$	$a = 0.5$	$a = 0.6$	$a = 1.0$
Local, $m = 1$	18%	7.0%	11%	2.7%
Local, $m = 2$	25%	2.6%	5.2%	0.26%
DtN, $N = 15$	0.011%	0.032%	0.024%	0.063%

Note. The artificial boundary is located at $\mu = a$, and the error is computed over the domain $\mu_0 \le \mu \le \mu_0 + 0.1$. The relative errors using the local boundary conditions (4.29) and the DtN condition (4.25) are shown for two different aspect ratios.

$$\frac{d}{d\xi}\left[(\xi^2-1)\frac{d}{d\xi}y\right]-\left(\lambda-c^2\xi^2+\frac{m^2}{\xi^2-1}\right)y=0. \quad (4.41)$$

Here $\lambda = \lambda_{mn}(c)$ is a separation constant, which reduces to $\lambda_{mn}(0) = n(n+1)$ in the spherical case.

The angular prolate spheroidal wave functions of the first kind are denoted by $S_{mn}^{(1)}(c, \cos\theta)$, $n \geq 0$, $0 \leq m \leq n$. They form an orthogonal set over the interval $0 \leq \theta \leq 2\pi$. We normalize the angular functions as in [10], namely,

$$\int_{-1}^{1}[S_{mn}^{(1)}(c,\eta)]^2\,d\eta=\frac{2}{2n+1}\frac{(n+m)!}{(n-m)!}. \quad (4.42)$$

Next, we let

$$m_{jn}(\theta,\phi,\theta',\phi')=S_{jn}^{(1)}(c,\cos\theta)S_{jn}^{(1)}(c,\cos\theta')\cos j(\phi-\phi') \quad (4.43)$$

and define the constants

$$\beta_{jn}=\frac{(2n+1)(n-j)!}{2\pi(n+j)!}. \quad (4.44)$$

We write the solution to the exterior radiation problem in the region $\mu \geq a$ as

$$U(\mu,\theta,\phi)=\sum_{n=0}^{\infty}{\sum_{j=0}^{n}}'\beta_{jn}\frac{R_{jn}^{(3)}(c,\cosh\mu)}{R_{jn}^{(3)}(c,\cosh a)} \int_{\mathcal{S}}U(a,\theta',\phi')m_{jn}(\theta,\phi,\theta',\phi')\,d\mathcal{S}'. \quad (4.45)$$

The prime after the sum indicates that terms with $j = 0$ are multiplied by $\frac{1}{2}$. To get the DtN condition at $\mu = a$, we differentiate (4.45) with respect to μ and set $\mu = a$. It is

$$\partial_\mu U(a,\theta,\phi) =\sum_{n=0}^{\infty}{\sum_{j=0}^{n}}'Z_{jn}\int_{\mathcal{S}}U(a,\theta',\phi')m_{jn}(\theta,\phi,\theta',\phi')\,d\mathcal{S}', \quad (4.46)$$

with

$$Z_{jn}=\frac{\beta_{jn}\sinh a\,R_{jn}^{(3)\prime}(c,\cosh a)}{R_{jn}^{(3)}(c,\cosh a)}. \quad (4.47)$$

To modify (4.46) we must first construct a local boundary condition. It was shown recently by Holford [11] that the solution U admits the multipole expansion

$$U=\frac{e^{ik\xi}}{k\xi}\sum_{j=0}^{\infty}\frac{f_j(\theta,\phi;k)}{(k\xi)^j}. \quad (4.48)$$

The series converges absolutely and uniformly for $\xi \geq \cosh a$, and it can be differentiated term by term. It is *formally* identical to the series used in [2], with r replaced by $f\xi$. By replacing r in (4.11) by $f\xi$, we obtain the analogous sequence of local operators

$$B_m=\prod_{l=1}^{m}\left(\frac{\partial}{f\partial\xi}-ik+\frac{2l-1}{f\xi}\right), \quad m\geq 1, \quad (4.49)$$

where $l = 1$ is the rightmost term in the product. The operator B_m annihilates the first m terms in (4.48). We can use it to construct the local boundary condition

$$B_m U = 0. \quad (4.50)$$

The derivation of the first modified DtN condition is similar to previous analyses and yields

$$\partial_\mu U(a,\theta,\phi)=(ikf\sinh a-\tanh a)\,U(a,\theta,\phi) +\sum_{n=0}^{N}{\sum_{j=0}^{n}}'Z_{jn}\int_{\mathcal{S}}U(a,\theta',\phi')m_{jn}(\theta,\phi,\theta',\phi')d\mathcal{S}', \quad (4.51)$$

with

$$Z_{jn}=\frac{\beta_{jn}\sinh a\,R_{jn}^{(3)\prime}(c,\cosh a)}{R_{jn}^{(3)}(c,\cosh a)}-ikf\sinh a+\tanh a. \quad (4.52)$$

To derive the second modified DtN condition, we rewrite $B_2U = 0$ at $\mu = a$ as $\partial_\mu U = BU$, with $B = (\partial_\mu^2 + (\alpha+1)\partial_\mu + \beta)U$. Here

$$\alpha = 4\tanh a-\coth a-2ikf\sinh a, \quad (4.53)$$

$$\beta = 2\tanh^2 a-(kf\sinh a)^2-4ikf\tanh a\sinh a. \quad (4.54)$$

Next, we add BU to the right side of (4.46) and then subtract it, including the subtracted term in the sum. We use (4.41) to evaluate $R_{mn}^{(3)\prime\prime}(c,\cosh\mu)$ and obtain the modified DtN condition

$$\partial_\mu U(a,\theta,\phi)=BU(a,\theta,\phi)+\sum_{n=0}^{N}{\sum_{j=0}^{n}}'\beta_{jn}Z_{jn} \int_{\mathcal{S}}U(a,\theta',\phi')m_{jn}(\theta,\phi,\theta',\phi')\,d\mathcal{S}'. \quad (4.55)$$

Here the constants Z_{jn} are given by

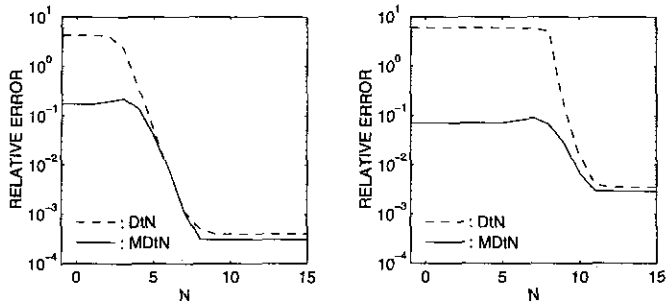

FIG. 5. Scattering of a plane wave from the prolate spheroid $\mu = 0.1$ of aspect ratio 10 : 1. The artificial boundary is located at $\mu = 0.5$. The relative error (4.1) is shown versus the truncation point N in the boundary conditions (4.46) and (4.55): left, $k = 2\pi$; right, $k = 4\pi$.

$$Z_{jn} = \frac{(\coth a - \alpha)\sinh a\, R_{jn}^{(3)\prime}(c, \cosh a)}{R_{jn}^{(3)}(c, \cosh a)} + c^2 \cosh^2 a - \lambda_{jn} - \frac{j^2}{\sinh^2 a} - \beta, \tag{4.56}$$

with α and β given by (4.53) and (4.54).

We note that it is easy to derive corresponding boundary conditions for oblate spheroidal coordinates, since the two coordinate systems are simply related by the transformations $\xi \to i\xi$, $c \to -ic$, and $\xi = \sinh \mu$. Moreover, a multipole expansion similar to (4.48) was developed in [11] for oblate spheroidal coordinates. Thus in oblate spheroidal coordinates, both the DtN condition and the corresponding sequence of local boundary operators can be obtained from (4.46) and (4.49) by performing this simple change of variables.

We now consider the scattering of a plane wave $U^i = e^{ikx}$ from a prolate spheroid, whose elliptic cross section is a confocal ellipse with foci located at $(\pm 1, 0, 0)$. We let $\mu_0 = 0.1$, so that the aspect ratio of major to minor axes is about 10 : 1. The incident direction is along the x-axis, which coincides with the major axis of the spheroid. The radial and the angular spheroidal wave functions are computed using [12, 13]. In Fig. 5 we compare the relative error obtained by using the DtN condition (4.46) truncated at N with that obtained by using the modified DtN condition (4.55) for different values of N. For $N = -1$, the DtN condition reduces to $\partial_\mu U = 0$, whereas the modified DtN condition reduces to (4.50) with B_2 given by (4.49). Again the error using the modified DtN condition is much smaller than that obtained using the truncated DtN condition for small values of N. It then decreases as N increases. The error using the truncated DtN condition remains large for small N, but then decreases very rapidly to reach its optimal value.

Next, we vary the aspect ratio of the spheroid $\mu = \mu_0$. In Table II we compare the performance of various boundary conditions for the two aspect ratios 10 : 1 and 2 : 1. This table is similar to Table I, and the discussion in the last paragraph of Section 4.4 applies to Table II as well.

TABLE II

Scattering of a Plane Wave from the Prolate Spheroid $\mu = \mu_0$ with $k = 2\pi$

	$\mu_0 = 0.1$, Aspect ratio 10 : 1		$\mu_0 = 0.5$, Aspect ratio 2 : 1	
$\mu = a$	$a = 0.2$	$a = 0.5$	$a = 0.6$	$a = 1.0$
Local, $m = 1$	38%	13%	18%	5.5%
Local, $m = 2$	44%	7.4%	8.5%	0.70%
DtN, $N = 15$	0.035%	0.033%	0.022%	0.064%

Note. The artificial boundary is located at $\mu = a$, and the error is computed over the domain $\mu_0 \le \mu \le \mu_0 + 0.1$. The relative errors using the local boundary conditions (4.46) and the DtN condition (4.49) are shown for two different aspect ratios.

5. IMPROVED LOCAL BOUNDARY CONDITIONS

The DtN and modified DtN boundary conditions are nonlocal in space, because they involve inner products over the whole artificial boundary S. The BGT [2], the Engquist–Majda [14], and the Kang [15] boundary conditions are local. To achieve convergence to the exact solution for a fixed location of S, one must gradually increase the order of derivatives that appear in the local boundary condition, as one refines the mesh. Otherwise, the numerical solution will not converge to the restriction to Ω of the exact solution. Instead, it will converge to the solution of a different problem, which satisfies the local boundary condition. In comparison, the DtN condition can be made arbitrarily accurate by increasing the value of N, without taking higher derivatives or increasing the size of Ω. This is clearly illustrated in Table III, where we see that the error for the DtN method steadily decreases by a factor of 4 as we halve both Δr and $\Delta\theta$. The error of the solution using the local boundary conditions (4.11) is barely reduced as we refine the grid. This indicates that the error introduced at the artificial boundary dominates the discretization error. However, a key advantage of local boundary conditions is that they do not require S to be a separable coordinate surface. We shall now derive a new sequence of local boundary conditions in two dimensions, which can be used at any artificial boundary S.

TABLE III

Scattering of a Plane Wave from the Sphere $r = 0.5$, with $k = 2\pi$ and the Artificial Boundary Located at $r = 1$

Grid size	BGT, $m = 1$	BGT, $m = 2$	DtN, $N = 15$
10×60	19%	2.7%	1.7%
20×120	18%	1.6%	0.43%
40×240	17%	1.4%	0.11%

Note. The relative error (4.1) is shown for the BGT local boundary conditions (4.11) and the DtN global boundary condition (4.15) as the grid is refined.

The local boundary conditions (4.3) were obtained in [2] using an asymptotic expansion of the solution U for large values of kr. This explains their rather poor performance for small values of ka. We shall now derive a new sequence of local boundary conditions based on an expansion due to Karp [16], namely,

$$U(r, \theta) \simeq H_0^{(1)}(kr) \sum_{n=0}^{\infty} \frac{F_n(\theta)}{r^n} + H_1^{(1)}(kr) \sum_{n=0}^{\infty} \frac{G_n(\theta)}{r^n}. \quad (5.1)$$

This series converges uniformly and absolutely for $r \geq a$ and may be differentiated termwise with respect to r as often as desired. We do not expand the two Hankel functions $H_0^{(1)}$ and $H_1^{(1)}$ for large values of kr, as was done in [2]. Instead, we construct a sequence of differential operators L_n,

$$L_0 = (\partial_r^2 + C_0 \partial_r + D_0), \quad (5.2)$$

$$L_n = (\partial_r^2 + C_n \partial_r + D_n) L_{n-1}, \quad n = 1, 2, \ldots, \quad (5.3)$$

which annihilate all terms in (5.1) up to and including r^{-n} (see also [17]). We then apply the boundary condition

$$L_n U = 0 \quad (5.4)$$

at the outer boundary S.

To construct L_0, we apply it to both $H_0^{(1)}(kr)$ and $H_1^{(1)}(kr)$ and require that the result be zero. This immediately gives

$$C_0 = \frac{1}{r} + \frac{1}{kr^2} \left(\frac{H_0^{(1)\prime}(kr)}{H_0^{(1)}(kr)} - \frac{H_1^{(1)\prime}(kr)}{H_1^{(1)}(kr)} \right)^{-1}, \quad (5.5)$$

$$D_0 = k^2 - \frac{1}{r^2} \left(1 - \frac{H_0^{(1)}(kr) H_1^{(1)\prime}(kr)}{H_0^{(1)\prime}(kr) H_1^{(1)}(kr)} \right)^{-1}. \quad (5.6)$$

By construction, we see that $L_0 U(r, \theta) = \mathbb{O}((kr)^{-(2+1/2)})$. Since B_2 is based upon an asymptotic expansion of the solution for large values of kr, it is clear that L_0 will approach B_2 asymptotically for large kr. This is illustrated in Fig. 6, where we have kept the outer radius fixed at $a = 1$, while increasing k.

We note that L_0 coincides with the localized second-order DtN operator presented in [18]. This is because L_0 is the unique second-order differential operator that annihilates both $H_0^{(1)}$ and $H_1^{(1)}$. But L_1 does not coincide with the fourth-order localized DtN operator. Indeed the latter annihilates $H_0^{(1)}$, $H_1^{(1)}$, $H_2^{(1)}$, and $H_3^{(1)}$, whereas the former annihilates $H_0^{(1)}$, $H_0^{(1)}/r$, $H_1^{(1)}$, and $H_1^{(1)}/r$. Thus, they must differ since $H_3^{(1)}$ cannot be written as a linear combination of $H_0^{(1)}$, $H_0^{(1)}/r$, $H_1^{(1)}$, and $H_1^{(1)}/r$.

We now compare the relative error (4.1) in the solution using the BGT boundary conditions (4.3) with $m = 1, 2$, with the error when the local boundary condition (5.4) with $n = 0$ is used. The artificial boundary is located at $r = a$ with $a = 1$, and we let k range from 0.01 up to 10. In Fig. 6 we see that

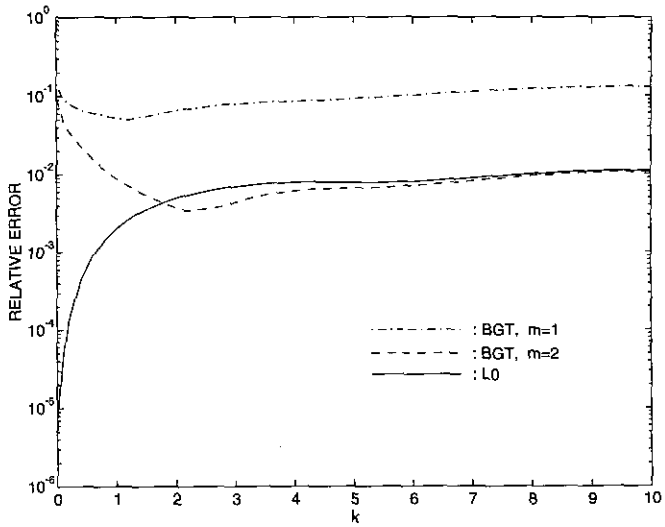

FIG. 6. Scattering of a plane wave from a circular cylinder of radius $r = 0.5$. The relative error (4.1) for various local boundary conditions imposed on $r = 1$ is shown versus the wave number k.

for small values of k the solution obtained with (5.4) is several orders of magnitude more accurate than that obtained with the two boundary conditions (4.3). For larger values of k the errors obtained with L_0 and the BGT condition with $m = 2$ become equal, as is to be expected, since they have the same asymptotic behavior for large values of ka. Although the relative error for L_0 is slightly larger for medium frequencies, this discrepancy is problem dependent and is clearly overemphasized by the logarithmic scale of the graph. We note that unlike the BGT condition (4.3) with $m = 2$, the relative error for L_0 remains smaller than 1% for all values of k.

6. CONCLUDING REMARKS

A. We have presented a modification of the truncated DtN boundary condition. It ensures well-posedness of the boundary value problem in the computational domain for all wave numbers, and in general improves upon the accuracy. Although we have presented the modified DtN condition only for the Helmholtz equation, our procedure applies to other equations for which DtN boundary conditions have been developed [19]. The modification procedure can also be applied to the exact nonreflecting boundary conditions that were obtained in [20] for the time-dependent wave equation in three space dimensions. We have also derived the DtN and modified DtN boundary conditions for elliptic and prolate spheroidal coordinates. Finally, we have presented several new sequences of local boundary conditions in circular, elliptic, and prolate spheroidal coordinates.

B. When the DtN boundary condition is truncated at mode N, two difficulties are introduced. The first is that the resulting problem in the bounded domain Ω will have eigenvalues of the

parameter ka. Then the problem in Ω is not uniquely solvable if ka is an eigenvalue, and it is ill-conditioned if ka is near an eigenvalue. The second difficulty is that for any value of ka, the solution will be inaccurate if $N < N_0$, where N_0 is the highest mode number in the exact solution of the problem considered. Both difficulties can be overcome by choosing N large enough. Ill-conditioning can be avoided by choosing $N \geq ka$, and inaccuracy can be avoided by choosing $N \geq N_0$. The modified DtN condition eliminates the first difficulty and mitigates the second one, even for small values of N.

C. Local boundary conditions, such as those of Bayliss, Gunzberger, and Turkel [2] and the improved conditions (5.4), can be used even when the artificial boundary is not a circle or sphere. However, the derivatives which appear in them must be *radial* derivatives with respect to some origin inside the artificial boundary. The coefficients in these conditions must be evaluated at the distance r from the origin to the artificial boundary, which will vary with position on the boundary. In general, the derivatives will not be normal to the artificial boundary, but will be combinations of normal and tangential derivatives. Similarly, the local boundary conditions (4.29) in elliptic coordinates and (4.50) in spheroidal coordinates can be used on any artificial boundary. The derivatives must be with respect to the radial coordinate μ in some appropriate elliptic or spheroidal coordinate system.

D. In modifying the DtN condition, we could use any local boundary condition. For example, in two dimensions when the artificial boundary is a circle, we could use either one of the BGT conditions (4.3), or one of the improved boundary conditions L_n given by (5.4), or one of the localized DtN conditions [18]. Our calculations, shown in Fig. 6, indicate that L_0 is better than the second BGT operator B_2 for small wave numbers. We have not used it to modify the DtN condition, because it is only better at small wave numbers, where even a few DtN terms provide adequate accuracy. Modifying the DtN operator is mainly intended to improve the boundary condition at high wave numbers. Any boundary operator based on the large distance expansion, such as B_m and L_n, can be used.

The DtN boundary condition can be modified with a first, second, or higher order local operator. A first-order operator leads to a well-posed problem for arbitrary obstacles at all wave numbers and, hence, yields a robust boundary condition. A second-order operator provides a more accurate boundary condition. Its implementation is straightforward if the finite difference method is used. To employ it with the finite element method, the second-order radial derivative must be expressed in terms of second-order tangential derivatives, which are then enforced weakly at the artificial boundary S. Higher order operators are more accurate but require a greater effort to implement. If the finite difference method is used, they extend the coupling between unknowns at S into Ω, which results in a linear system with a wider bandwidth. If the finite element method is used, these operators require special basis functions, which provide higher regularity than C^0 on S [21].

APPENDIX

We now derive the asymptotic expansion (4.26) of $U(\mu, \theta)$ for large μ. Let $\mu = a$ with $a > 0$ be the outer elliptic boundary. In the exterior domain $\mu \geq a$ the solution U is given by (4.24). The radial Mathieu–Hankel function $Mc_r^{(3)}$ admits the asymptotic expansion [6, Eq. (20.9.1) with $\nu = r$ and $\sigma = 0$]

$$Mc_r^{(3)}(\mu, q) \sim \frac{e^{i(2\sqrt{q}\cosh\mu - r\pi/2 - \pi/4)}}{\sqrt{\pi\sqrt{q}\cosh\mu}} \sum_{m=0}^{\infty} \frac{D_m(a_r)}{[-4i\sqrt{q}\cosh\mu]^m}. \quad \text{(A.1)}$$

The radial function $Ms_r^{(3)}$ admits the same expansion with r replaced by $-r$ and the right side multiplied by $(-1)^r$; then the constants D_m depend upon b_r. We recall that $\sqrt{q} = kf/2$, and we replace $Mc_r^{(3)}$ and $Ms_r^{(3)}$ in (4.24) by their respective asymptotic expansions (A.1). Next, we interchange the sums over r and m to obtain

$$U(\mu, 0) \sim \sqrt{2/\pi kf\cosh\mu}\, e^{i(kf\cosh\mu - \pi/4)} \sum_{m=0}^{\infty} \frac{g_m(\theta; k)}{[kf\cosh\mu]^m}. \quad \text{(A.2)}$$

Here $g_m(\theta; k)$ is defined by

$$g_m(\theta; k) = \sum_{r=0}^{\infty} \left[A_r e^{-ir\pi/2} ce_r(\theta, q) \frac{D_m(a_r)}{-2i} + B_r e^{ir\pi/2} se_r(\theta, q) \frac{D_m(b_r)}{-2i} \right], \quad \text{(A.3)}$$

where A_r and B_r are arbitrary constants.

ACKNOWLEDGMENTS

We thank Oliver Ernst for his Matlab code [5], A. L. Van Buren for the documentation and FORTRAN code for computing spheroidal wave functions [12, 13], and Dan Givoli for reading the manuscript.

REFERENCES

1. J. B. Keller and D. Givoli, *J. Comput. Phys.* **82,** 172 (1989).
2. A. Bayliss, M. Gunzburger, and E. Turkel, *SIAM J. Appl. Math.* **42**(2), 430 (1982).
3. I. Harari and T. J. R. Hughes, *Comput. Meth. Appl. Mech. Eng.* **97,** 103 (1992).
4. P. M. Morse and H. Feshbach, *Methods of Theoretical Physics* (McGraw–Hill, New York, 1953).
5. O. G. Ernst, Ph.D. dissertation, Scientific Computing and Computational Mathematics Program, Stanford University, October 1994; Report SCCM-95-01, Stanford University, January 1995.
6. M. Abramowitz and I. A. Stegun, *Handbook of Mathematical Functions,* Appl. Math. Series, Vol. 55 (National Bureau of Standards, Washington, DC, 1964).

7. R. B. Shirts, *ACM Trans. Math. Software* **19,** 391 (1993).
8. G. Blanch and D. S. Clemm, *Tables Relating to the Radial Mathieu Functions,* Vols. I, II (Aerospace Research Laboratories, USAF, 1965).
9. C. Flammer, *Spheroidal Wave Functions* (Stanford Univ. Press, Stanford, CA, 1956).
10. J. Meixner and F. W. Schäfke, *Mathieusche Funktionen und Sphäroidfunktionen* (Springer-Verlag, New York/Berlin, 1954).
11. R. L. Holford, *J.A.S.A.*, in press.
12. B. J. King, R. V. Baier, and S. Hanish, NRL Report 7012, March 1970 (unpublished).
13. B. J. Patz and A. L. Van Buren, NRL Memorandum Report 4414, March 1981 (unpublished).
14. B. Engquist and A. Majda, *Math. Comput.* **31**(139), 629 (1977).
15. F. Kang, *J. Comput. Math.* **2**(2), 130 (1984).
16. S. N. Karp, *Commun. Pure Appl. Math.* **14,** 427 (1961).
17. A. Bayliss and E. Turkel, *J. Comput. Phys.* **48,** 182 (1982).
18. D. Givoli and J. B. Keller, *Wave Motion,* **12,** 261 (1990).
19. D. Givoli, *Numerical Methods for Problems in Infinite Domains,* Studies in Appl. Mech., Vol. 33 (Elsevier, Amsterdam, 1992).
20. M. Grote and J. B. Keller, *SIAM J. Appl. Math.*, **April** (1995).
21. D. Givoli and J. B. Keller, *Comput. Methods Appl. Mech. Eng.* **119,** 199 (1994).